



# Lattice QCD Studies of the Leading Order Hadronic Contribution to the Muon $g - 2$

Anthony Francis<sup>a</sup>, Vera Gülpers<sup>a,b</sup>, Gregorio Herdoíza<sup>c</sup>, Georg von Hippel<sup>a</sup>, Hanno Horch<sup>a</sup>, Benjamin Jäger<sup>d</sup>, Harvey B. Meyer<sup>a,b</sup>, Eigo Shintani<sup>a</sup>, Hartmut Wittig<sup>a,b</sup>

<sup>a</sup>PRISMA Cluster of Excellence, Institut für Kernphysik,  
Johannes Gutenberg-Universität, 55099 Mainz, Germany

<sup>b</sup>Helmholtz Institute Mainz,

Johannes Gutenberg-Universität, 55099 Mainz, Germany

<sup>c</sup>Instituto de Física Teórica UAM/CSIC and Departamento de Física Teórica,  
Universidad Autónoma de Madrid, Cantoblanco, E-28049 Madrid, Spain

<sup>d</sup>Department of Physics, Swansea University, Swansea, United Kingdom

## Abstract

The anomalous magnetic moment of the muon,  $g_\mu - 2$ , is one of the most promising observables to identify hints for physics beyond the Standard Model. QCD contributions are currently responsible for the largest fraction of the overall theoretical uncertainty in  $g_\mu - 2$ . The possibility to determine these hadronic contributions from first principles through lattice QCD calculations has triggered a number of recent studies. Recent proposals to improve the accuracy of lattice determinations are reported. We present an update of our studies of the leading-order hadronic contribution to  $g_\mu - 2$  with improved Wilson fermions.

## Keywords:

muon  $g - 2$ , hadronic vacuum polarisation, lattice QCD

## 1. Introduction

The anomalous magnetic moment of the muon,  $a_\mu = (g_\mu - 2)/2$ , is a remarkable example of a quantity that can be studied with very high accuracy on both the experimental and the theoretical sides. The 0.5 ppm uncertainty of the current experimental value allows to probe contributions from electromagnetic, strong and weak interactions. The Standard Model (SM) prediction has reached a comparable precision [1],

$$a_\mu^{\text{th}} = 116\,591\,803(42)(26)(01) \cdot 10^{-11} [0.4 \text{ ppm}],$$
$$a_\mu^{\text{exp}} = 116\,592\,091(54)(33) \cdot 10^{-11} [0.5 \text{ ppm}]. \quad (1)$$

The deviation between theory and experiment currently amounts to a  $3.6 \sigma$  effect. The next generation of experiments at Fermilab [2] and J-PARC [3] aims at a reduction of the uncertainty in  $a_\mu$  by a factor of four. Such

a precision will substantially enhance the sensitivity to physics beyond the SM. It is, however, equally important to examine the reliability of the current SM prediction and to attempt to reduce its uncertainty to the level of the forthcoming experimental results. The SM result has recently profited from an outstanding achievement in determining the QED contribution up to 5-loop order [4]. Theory errors in eq. (1) arise from lowest-order hadronic (HLO), higher-order hadronic and electroweak contributions, respectively. The SM error is thus markedly dominated by QCD dynamics and, in particular, by HLO vacuum polarisation effects.

The HLO vacuum polarisation contribution,  $a_\mu^{\text{HLO}}$ , can be obtained by a dispersive approach that combines basic properties of the theory – such as analyticity and unitarity – with experimental input. A collection of recent measurements [5–7] of inclusive hadronic cross-sections,  $\sigma(e^+e^- \rightarrow \text{hadrons})$ , has allowed to

reach a 0.6% precision on the LO hadronic contribution,  $a_\mu^{\text{HLO}} = 6923(42) \cdot 10^{-11}$  [1]. A persistent  $\sim 3\sigma$  deviation between the analyses of the  $\pi^+\pi^-$  channel by BaBar and KLOE has an impact on the SM prediction. This is being investigated by several experiments [3]. Conversely, the tension in the results for  $a_\mu^{\text{HLO}}$  based on  $e^+e^-$  and  $\tau$  data has recently been reduced below the  $2\sigma$  level [7, 8].

Since the dispersion relation results largely depend on experimental data, it is desirable to consider also an independent approach based on first principles. A determination of  $a_\mu^{\text{HLO}}$  along these lines can be achieved through lattice QCD. A number of studies [9–15] have demonstrated the potential of this approach. It is nonetheless still a considerable challenge for the lattice studies to reach the sub-percent accuracy of the dispersion relation result. There has recently been an intense activity in order to devise new ways of improving the accuracy of the lattice determinations of  $a_\mu^{\text{HLO}}$ .

## 2. Lattice QCD Determinations of $a_\mu^{\text{HLO}}$

The hadronic vacuum polarisation tensor, depending on the Euclidean momentum  $Q$ , reads

$$\Pi_{\mu\nu}(Q) = \int d^4x e^{iQx} \langle J_\mu(x) J_\nu(0) \rangle, \quad (2)$$

where the flavour singlet vector current is given by,

$$J_\mu(x) = \sum_{f=u,d,s,c,\dots} Q_f \bar{\psi}_f(x) \gamma_\mu \psi_f(x). \quad (3)$$

$Q_f$  is the electric charge of the quark flavour  $f$ . Euclidean invariance and current conservation imply,

$$\Pi_{\mu\nu}(Q) = (Q_\mu Q_\nu - \delta_{\mu\nu} Q^2) \Pi(Q^2). \quad (4)$$

The VPF  $\Pi(Q^2)$  can be decomposed into non-singlet and singlet contributions. The subtracted VPF,  $\widehat{\Pi}(Q^2) = \Pi(Q^2) - \Pi(0)$ , is free of ultraviolet divergences and can be convoluted with a known analytic kernel function  $K(Q^2, m_\mu)$  to derive the *standard representation* for  $a_\mu^{\text{HLO}}$  [9, 16] currently being used on the lattice,

$$a_\mu^{\text{HLO}} = 4\alpha^2 \int_0^\infty dQ^2 K(Q^2, m_\mu) \widehat{\Pi}(Q^2), \quad (5)$$

where  $m_\mu$  is the muon mass. A comparison of lattice QCD determinations of  $a_\mu^{\text{HLO}}$  [11–15] is shown in Fig. 1. The present uncertainty from the lattice computations is larger than the 0.6% precision of the dispersion relation approach. With the current accuracy, it is still challenging to isolate the relative contributions from dynamical

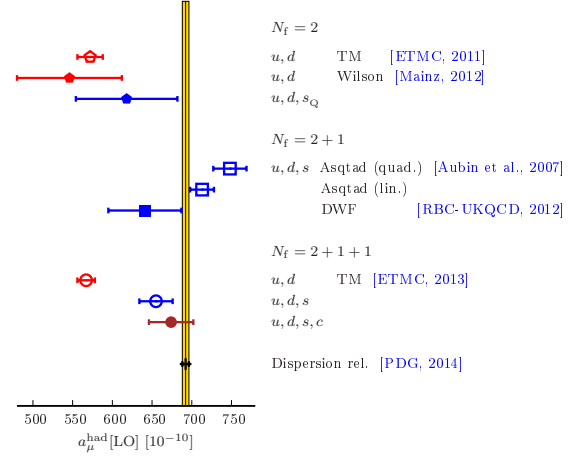


Figure 1: Comparison of lattice determinations of  $a_\mu^{\text{HLO}}$  [11–15]. The number of flavours in the sea is labelled by  $N_f$  while the flavour content in the valence sector, appearing in eq. (3), is denoted by  $u, d, s$  and  $c$ . The dispersion relation approach – with a 0.6% relative precision [1] – is denoted by the yellow vertical band.

strange and charm quarks. However, the  $s$  and  $c$  valence contributions – while being significantly smaller than those from  $u, d$  quark flavours – can be determined with relatively good precision [15, 17].

The uncertainties of the lattice QCD results of  $a_\mu^{\text{HLO}}$  have multiple origins. In the next section we outline the main sources of errors affecting these computations and report about the recent proposals to address them.

## 3. Behaviour of the VPF at Low $Q^2$

A crucial aspect of the computation of  $a_\mu^{\text{HLO}}$  is to constrain with accurate lattice data the  $Q^2$  region where the integrand in eq. (5) is large. In practice, this region is in the neighbourhood of  $Q^2 \approx m_\mu^2/4 \approx 0.003 \text{ GeV}^2$ . However, this low- $Q^2$  regime poses serious problems for lattice studies based on an evaluation of  $\Pi(Q^2)$  from eq. (4), since the transverse projector on the r.h.s vanishes at  $Q^2 = 0$ . In finite volume with periodic boundary conditions, the minimal momentum is quantised in units of the lattice size  $L$ , by  $Q_{\text{min}}^2 = (2\pi/L)^2$ . Directly probing the dominant region,  $Q^2 \approx m_\mu^2/4$ , would require values of  $L \approx 20 \text{ fm}$  that are far beyond what is achievable with present-day resources. Furthermore, in this small  $Q^2$  regime, long-distance QCD effects induce large fluctuations on the VPF. To illustrate these effects an auxiliary observable,  $\bar{a}_\mu^{\text{had}}(Q_{\text{ref}}^2)$ , is defined as follows,

$$\bar{a}_\mu^{\text{HLO}}(Q_{\text{ref}}^2) = 4\alpha^2 \int_{Q_{\text{ref}}^2}^\infty dQ^2 K(Q^2) [\Pi(Q^2) - \Pi(Q_{\text{ref}}^2)]. \quad (6)$$

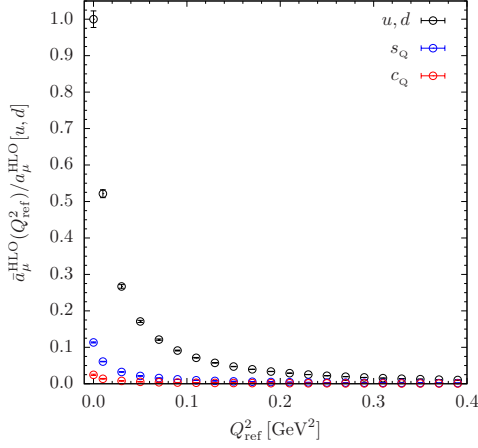


Figure 2: Momentum dependence of  $\bar{a}_\mu^{\text{HLO}}(Q_{\text{ref}}^2)$ , defined in eq. (6), and coinciding with  $a_\mu^{\text{HLO}}$  at  $Q_{\text{ref}}^2 = 0$ . The y-axis is normalised by  $a_\mu^{\text{HLO}}[u, d]$ . The region,  $Q_{\text{ref}}^2 \gtrsim 0.4 \text{ GeV}^2$ , is observed to contribute very little to  $a_\mu^{\text{HLO}}$ . When increasing the quark mass from the mass-degenerate  $u, d$  quark sector to the strange and charm regions, a strong suppression of the contribution to  $a_\mu^{\text{HLO}}$  is observed. The current accuracy however requires these various contributions to be included.

This quantity coincides with  $a_\mu^{\text{HLO}}$  in the limit  $Q_{\text{ref}}^2 \rightarrow 0$ . Fig. 2 shows the dependence of  $\bar{a}_\mu^{\text{HLO}}$  on  $Q_{\text{ref}}^2$ . The  $u, d$  valence quark contribution is dominated by the region  $Q_{\text{ref}}^2 \lesssim 0.4 \text{ GeV}^2$ . Moreover, the relative error on  $\bar{a}_\mu^{\text{HLO}}$  increases when reducing  $Q_{\text{ref}}^2$ . A clear hierarchy is observed in the size of the ( $u, d$ ),  $s$  and  $c$  valence contributions. In spite of that, the current accuracy is at a level that renders the inclusion of these effects appropriate. A number of ideas have been recently put forward to tackle the issue of reaching the small  $Q^2$  regime.

*Partially Twisted Boundary Conditions.* To circumvent the limitation of having access only to a restricted set of low momentum values, periodic boundary conditions for the valence quark fields can be replaced by twisted boundary conditions [18–20]. A denser set of momenta can thus be reached [14] in a region closer to  $Q^2 \approx m_\mu^2$ , at the price of additional numerical effort and of small systematic effects from the breaking of isospin symmetry [21–23]. The increasing fluctuations in  $\Pi(Q^2)$  at small  $Q^2$  values are however still present when adopting this procedure.

*Extrapolation to  $Q^2 = 0$ .* The integrand in eq. (5) is peaked at low  $Q^2$  where lattice data are not available. Moreover, an extrapolation of  $\Pi(Q^2)$  to  $Q^2 \rightarrow 0$  is needed when relying on the *standard representation* for  $a_\mu^{\text{HLO}}$ . The estimate of the systematic effects associated with this extrapolation is one of the crucial aspects of present lattice calculations. Parametrisations of the  $Q^2$

dependence of the VPF based on vector meson dominance can introduce a model dependence that is difficult to quantify. Alternatively, Padé approximants supply a model-independent and systematically improvable description of the  $Q^2$  behaviour of  $\Pi(Q^2)$  [14, 24, 25]. Correlations among  $Q^2$  data points and the increasing number of fit parameters limits the order of the Padé approximants that can be reached for the purpose of testing the convergence properties of the series. This problem can be alleviated by restricting the use of Padé fits to the low momentum region,  $Q^2 \lesssim 0.4 \text{ GeV}^2$ , which is known to provide the bulk on the contribution to  $a_\mu^{\text{HLO}}$ , see Fig. 2. By splitting the bounds of the integral in eq. (5) into low and high  $Q^2$  intervals, a dedicated analysis of each of these regions can lead to an additional handle on the assessment of systematic effects [26, 27].

*Momentum Derivatives of the Vacuum Polarisation.* A complementary way to scrutinise the difficulties encountered in the low- $Q^2$  region is to consider derivatives with respect to momentum of the vacuum polarisation.

By applying derivatives of the vacuum polarisation tensor in eq. (4) with respect to  $Q_\mu$  and  $Q_\nu$ , it is possible to extract  $\Pi(Q^2)$  and, in particular, to isolate  $\Pi(0)$ . These derivatives have formally been applied in order to rewrite  $\Pi(0)$  in terms of suitable correlation functions involving the integrated insertion of currents [28]. The availability of  $\Pi(0)$  then allows to reach the dominant momentum region,  $Q^2 \approx m_\mu^2$ , through an interpolation.

The derivative of the VPF with respect to  $Q^2$  is free of ultraviolet divergences. The Adler function [29, 30] is a related physical quantity, defined as follows,

$$D(Q^2) = 12\pi^2 Q^2 \frac{d\Pi(Q^2)}{dQ^2}. \quad (7)$$

The Adler function can be combined with an appropriate kernel function to derive an alternative representation for  $a_\mu^{\text{HLO}}$  [31, 32],

$$a_\mu^{\text{HLO}} = \frac{\alpha^2}{6\pi^2} \int_0^1 dx \frac{(1-x)(2-x)}{x} D\left(\frac{x^2 m_\mu^2}{1-x}\right), \quad (8)$$

where the substitution  $Q^2 \rightarrow x^2 m_\mu^2 / (1-x)$  was applied. In this way, lattice determinations of  $D(Q^2)$  [21, 33, 34] can be used to directly compute  $a_\mu^{\text{HLO}}$  [35].

The idea of taking the derivative of  $\Pi(Q^2)$  with respect to  $Q^2$  can be extended to include higher order derivatives at  $Q^2 = 0$ , computed via Euclidean-time moments of the vector correlation function, eq. (10), at vanishing spatial momentum [17]. The subtracted VPF can then be constructed from its Taylor expansion. Long-distance effects are enhanced when increasing the order

of the moments. For the  $u, d$  contribution, these effects are expected to be sizeable since they are related to the two-pion decay channel of the  $\rho$ -meson.

A new integral representation for  $a_\mu^{\text{HLO}}$  based on the Mellin transform of the hadronic spectral function [36] relies on the calculation of the moments  $\mathcal{M}(-n)$ ,

$$\mathcal{M}(-n) = \frac{(-1)^{n+1}}{(n+1)!} (m_\mu^2)^{n+1} \frac{d^{n+1}}{(dQ^2)^{n+1}} \widehat{\Pi}(Q^2) \Big|_{Q^2=0}, \quad (9)$$

with  $n = \{0, 1, 2, \dots\}$ . In this approach, the subtracted VPF also appears in the evaluation of integrals over  $Q^2$ , which are, however, better suited than e.g. eq. (5) for the regime of momenta accessible on the lattice. An evaluation based on a phenomenological model [37] indicates that already for the order  $n = 3$ , a 1% deviation from a determination of  $a_\mu^{\text{HLO}}$  based on the dispersion relation approach could be achieved [36].

*Mixed (Time-Momentum) Representation.* Different representations for  $a_\mu^{\text{HLO}}$  can provide alternative means to monitor the leading systematic effects present in lattice computations – a few examples have been mentioned above. These integral representations can differ by the weight given to the integrand by a particular  $Q^2$  region or by the relative size of the long-distance contributions. A representation could thus be better suited for lattice QCD studies provided that it is more constrained by the region where data is available and sufficiently accurate.

A *mixed-representation* of the subtracted VPF involving the time-momentum dependence of the vector correlation function  $G(x_0, \vec{k})$ ,

$$G(x_0, \vec{k}) = \int d^3x e^{i\vec{k}\vec{x}} \langle J_\mu(x_0, \vec{x}) J_\mu(0) \rangle, \quad (10)$$

can be written as follows [37],

$$\widehat{\Pi}(Q^2) = \int_0^\infty dx_0 G(x_0, \vec{k} = 0) \left[ x_0^2 - \frac{4}{Q^2} \sin^2 \left( \frac{1}{2} Q x_0 \right) \right]. \quad (11)$$

The subtracted VPF determined in this way preserves a continuous dependence on  $Q^2$ , in particular in the neighbourhood of  $Q^2 = 0$  [34, 38, 39].

The integration bounds in eq. (11) imply that long-distance effects in  $G(x_0, \vec{k} = 0)$  will contribute. For  $u, d$  quarks, they are governed by the resonance nature of the  $\rho$ -meson. This necessitates the incorporation of interpolating operators which couple efficiently to two-pion states into the vector correlation function. An appealing feature of the mixed-representation is that quark-disconnected diagrams, which arise from the singlet contribution to the vector correlation function, can

Ens.	$a$ [fm]	$V/a^4$	$M_\pi$	$M_\pi L$	$N_{\text{meas}}$
A3	0.079	$64 \times 32^3$	473	6.0	1004
A4		$64 \times 32^3$	363	4.7	1600
A5		$64 \times 32^3$	312	4.0	1004
B6		$96 \times 48^3$	267	5.1	1224
E5	0.063	$64 \times 32^3$	456	4.7	4000
F6		$96 \times 48^3$	325	5.0	1200
F7		$96 \times 48^3$	277	4.2	1000
G8		$128 \times 64^3$	193	4.0	820
N5	0.050	$96 \times 48^3$	430	5.2	1392
N6		$96 \times 48^3$	340	4.1	2236
O7		$128 \times 64^3$	261	4.4	552

Table 1: Ensembles of  $O(a)$  improved Wilson fermions used in the determination of  $a_\mu^{\text{HLO}}$  by the Mainz group. Approximate values of the lattice spacing  $a$  and of the pion mass  $M_\pi$  (in MeV) together with information about the lattice volume and the number of measurements  $N_{\text{meas}}$  are given.

be evaluated straightforwardly using efficient noise reduction techniques [40].

Since different representations can lead to an improved control of the uncertainties in distinct  $Q^2$  intervals, it is beneficial to combine the use of these representations to reduce the overall error on  $a_\mu^{\text{HLO}}$ . In general, a mixture of methods based on previously discussed ideas – used in combination with variance reduction techniques [41, 42] – is expected to lead to a more accurate lattice result for  $a_\mu^{\text{HLO}}$ .

#### 4. Reaching the Physical Point

We already mentioned that various sea and valence quark flavours contributing to  $a_\mu^{\text{HLO}}$  are now being incorporated in the lattice simulations (see Fig. 1). In addition, simulations with non-degenerate  $u$  and  $d$  quark masses [22] or studies of the valence  $b$ -quark contribution with NRQCD [43] are also being considered.

The approach to the physical point in the  $u, d$  sector can be a source of sizeable systematic effects. The light-quark mass dependence of  $a_\mu^{\text{HLO}}$  is linked to the resonance nature of the  $\rho$ -meson and is thus expected to become more important when approaching the chiral limit. Different fit forms, often inspired by chiral effective theories, have been used to estimate the uncertainty from the chiral extrapolation. The explicit measurement of the vector meson mass has also been used in the calculation of  $a_\mu^{\text{HLO}}$  to modify its chiral behaviour [12]. Studies including simulations in the neighbourhood of the physical point have recently been reported [17, 22, 44]. For sufficiently large volumes, the physical effect of the  $\rho$ -

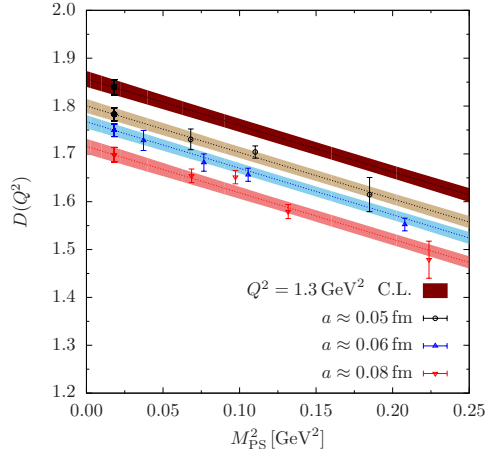


Figure 3: Pion-mass dependence of the Adler function  $D(Q^2)$  at fixed  $Q^2 = 1.3 \text{ GeV}^2$ . The upper band, denoted by ‘C.L.’ in the legend, is the continuum limit estimate. The leftmost (filled) symbols refer to the extrapolated values at the physical pion mass.

meson decay will contribute and a dedicated effort will be needed to address the associated fluctuations.

## 5. Studies of $a_\mu^{\text{HLO}}$ with improved Wilson fermions

The lattice group in Mainz has developed a dedicated research program aiming at a precise determination of physical observables related to the VPF [14, 21, 34, 35, 39, 40, 42, 45, 47, 48]. We report some recent developments in the study of  $a_\mu^{\text{HLO}}$  where several of the previously discussed advances have been implemented.

The lattice QCD ensembles (c.f. table 1) with two dynamical flavours of non-perturbatively  $O(a)$  improved Wilson fermions were produced as part of the CLS initiative. They include three values of the lattice spacing  $a$ , large volumes and pion masses down to  $M_\pi \approx 190 \text{ MeV}$ . A substantial increase in the number of measurements  $N_{\text{meas}}$  has also been achieved recently.

The VPF is extracted through eq. (4) from a lattice determination of the vacuum polarisation tensor, using local-conserved vector currents in the r.h.s of eq. (2). A high density of  $Q^2$  points for the VPF is attained by the use of partially twisted boundary conditions. We take advantage of this in order to derive the Adler function  $D(Q^2)$  in eq. (7) from numerical derivatives of the VPF [21, 35]. The  $Q^2$  dependence of the Adler function is then analysed in terms of Padé approximants of various orders. This study is integrated into a global analysis of  $D(Q^2)$  combining all the ensembles listed in table 1. An estimate of  $D(Q^2)$  in the continuum limit and at the physical point can be obtained in this way.

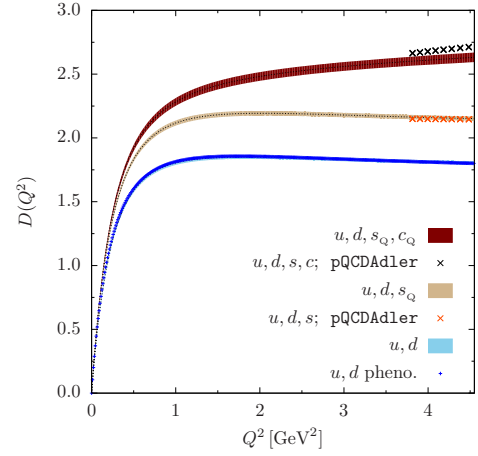


Figure 4: Contributions from  $(u, d)$  and from partially quenched strange  $s_Q$  and charm  $c_Q$  quark flavours to the Adler function after having performed the continuum and chiral extrapolations. The  $(u, d)$  contribution shows a good agreement with the phenomenological model of ref. [37] denoted by the blue ‘+’ symbols. For the cases where  $s_Q$  and  $c_Q$  are included, a comparison to perturbative QCD results from the pQCDAdler package [46] is shown.

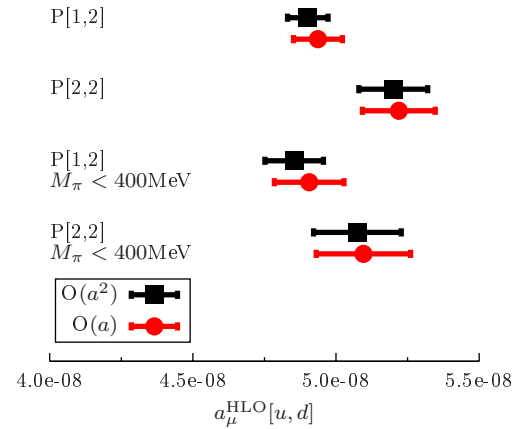


Figure 5: Preliminary results for the  $u, d$  contribution to  $a_\mu^{\text{HLO}}$  based on the determination of the Adler function and on the use of the representation in eq. (8). The  $Q^2$  dependence is examined by the use of Padé approximants of order [1, 2] and [2, 2]. Fits where pion masses,  $M_\pi \geq 400 \text{ MeV}$ , have been included/excluded are used to study systematic effects in the light-quark mass dependence of  $a_\mu^{\text{HLO}}$ . We observe that lattice artefacts are under control by performing separate analyses with fit ansätze including either  $O(a)$  or  $O(a^2)$  terms [35].

An illustration of the pion-mass dependence of the non-singlet  $(u, d)$  contribution to the Adler function at fixed  $Q^2$  is shown in Fig. 3. Systematic effects due to lattice artefacts and from the extrapolation of the light-quark mass to the physical point are explored by considering various fit forms and by repeating the analysis on subsets of the available ensembles [35]. The light  $(u, d)$  as well as the partially quenched strange  $s_Q$  and charm  $c_Q$

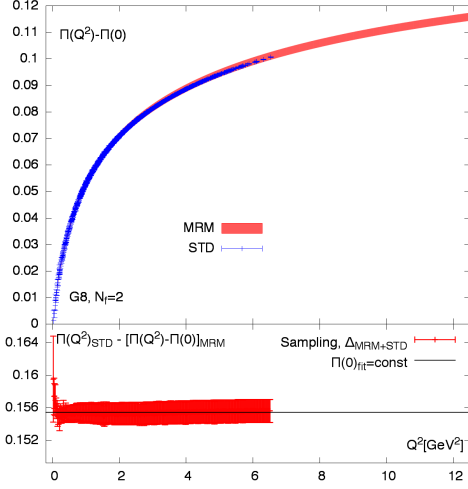


Figure 6: Comparison of the determinations of the subtracted VPF from the mixed-representation method (MRM) in eq. (11) and from the more standard approach (STD) based in eq. (4) and an extrapolation of  $\Pi(Q^2)$  to  $Q^2 = 0$ . The upper panel shows the consistency among these methods for  $\widehat{\Pi}(Q^2)$  over a large  $Q^2$  interval. The lower panel shows the corresponding difference,  $\Pi(Q^2)_{\text{STD}} - \widehat{\Pi}(Q^2)_{\text{MRM}}$  and demonstrates the stability of the derived values of  $\Pi(0)$ . Data from an ensemble with  $M_\pi \approx 190$  MeV are shown but similar results are observed for heavier pion masses up to  $\sim 450$  MeV [39].

contributions to  $D(Q^2)$  are displayed in Fig. 4. Some interesting applications of the Adler function include the matching to perturbation theory to determine the QCD coupling constant  $\alpha_s$  or the study of the hadronic contribution to the running of QED coupling [47, 48]. Preliminary results for  $a_\mu^{\text{HLQ}}$  from the use of the Adler function representation in eq. (8) are shown in Fig. 5.

The determination of the subtracted VPF from the *mixed-representation* in eq. (11) can be compared to the more standard procedure where  $\Pi(Q^2)$  is extracted from eq. (4) and then extrapolated to  $Q^2 = 0$  to determine  $\widehat{\Pi}(Q^2)$  [39]. The top panel of Fig. 6 shows an example of this comparison for the subtracted VPF over a large  $Q^2$  interval. The agreement is corroborated by the lower panel of Fig. 6 where the extrapolated estimate for  $\Pi(0)$  is checked against the mixed-representation method.

The flavour singlet currents in eq. (3) require the presence of Wick contractions involving both quark-connected and quark-disconnected contributions to the vector correlation functions. The latter suffer from large statistical fluctuations and are therefore often neglected in present lattice computations due to their high computational cost. It is however crucial to put a bound on their expected size. The *mixed-representation* correlator  $G(x_0, \vec{k} = 0)$  in eq. (10) is dominated in the large Euclidean time limit by the lowest energy state corre-

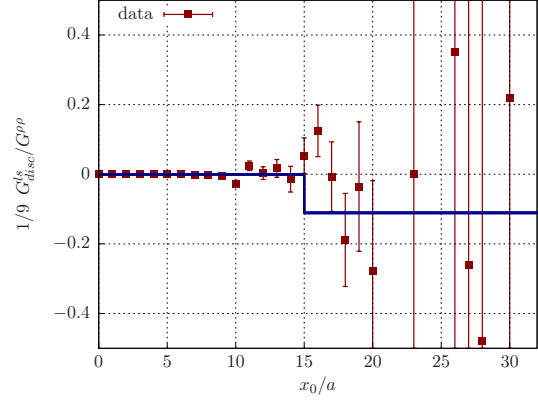


Figure 7: Lattice evaluation of the Euclidean time dependence of the ratio of the quark-disconnected vector correlation  $G_{\text{disc}}^{\ell s}(x_0)$ , involving light  $\ell = u, d$  and strange  $s$  quarks, to the isovector  $\rho$ -meson correlation function  $G^{\rho\rho}(x_0)$  [40]. The asymptotic value  $-1/9$  in eq. (12) is denoted by the blue horizontal line for  $x_0/a \geq 15$ . Approximately  $4 \cdot 10^5$  inversions of the Dirac operator are needed to achieve the accuracy shown in this figure.

sponding to the isovector channel, i.e.  $G^{\rho\rho}(x_0)$ . This leads to the following asymptotic behaviour [34, 40] of the quark-disconnected vector correlation  $G_{\text{disc}}^{\ell s}(x_0)$  involving light  $\ell = u, d$  and strange  $s$  quarks,

$$\frac{1}{9} \frac{G_{\text{disc}}^{\ell s}(x_0)}{G^{\rho\rho}(x_0)} \xrightarrow{x_0 \rightarrow \infty} -\frac{1}{9}, \quad (12)$$

in agreement with the expectation based on ChPT [49]. A lattice evaluation of the l.h.s. of eq. (12) as a function of  $x_0$  is shown in Fig. 7. A significant reduction of the statistical fluctuations in  $G_{\text{disc}}^{\ell s}(x_0)$  was obtained by using the same stochastic sources for the light and strange quark contributions. The signal is compatible with zero with an error approaching  $1/9$  at  $x_0 \approx 15a \approx 1$  fm. By assuming that the asymptotic value in eq. (12) is reached at this distance, a conservative upper bound on the disconnected contribution of  $\sim 4\%$  can be inferred.

## Conclusions

In the next few years, a new generation of experiments is expected to improve the determination of the anomalous magnetic moment of the muon  $a_\mu$  by a factor of four. A similar improvement in the SM prediction would greatly enhance the sensitivity to physics beyond the SM. Leading order hadronic effects are responsible for the largest theoretical uncertainty in  $a_\mu$ , coming from a phenomenological approach based on a combination of dispersive techniques and experimental data. Lattice QCD provides a first principles determination that can

lead to an independent and valuable check. We have presented some recent ideas and applications that are expected to lead to an improved determination of  $a_\mu^{\text{HLO}}$ . Higher-order hadronic effects from light-by-light scattering are the second largest source of error in the SM prediction of  $a_\mu$ . We refer to ref. [50] for a review presented at this conference about the recent progress in using lattice QCD to determine these contributions.

## Acknowledgements

We thank Michele Della Morte, Andreas Jüttner and Andreas Nyffeler for useful discussions. Our calculations were performed on the “Wilson” and “Clover” HPC Clusters at the Institute of Nuclear Physics, University of Mainz. We thank Dalibor Djukanovic and Christian Seiwerth for technical support. This work was granted access to the HPC resources of the Gauss Center for Supercomputing at Forschungszentrum Jülich, Germany, made available within the Distributed European Computing Initiative by the PRACE-2IP, receiving funding from the European Community’s Seventh Framework Programme (FP7/2007-2013) under grant agreement RI-283493 (project PRA039). We are grateful for computer time allocated to project HMZ21 on the BG/Q JUQUEEN computer at NIC, Jülich. This research has been supported in part by the DFG in the SFB 1044. We thank our colleagues from the CLS initiative for sharing the ensembles used in this work. G.H. acknowledges support by the Spanish MINECO through the Ramón y Cajal Programme and through the project FPA2012-31686 and by the Centro de Excelencia Severo Ochoa Program SEV-2012-0249.

## References

- [1] K. A. Olive *et al.* [PDG Collaboration], *Chin. Phys. C* **38** (2014) 090001.
- [2] R. M. Carey *et al.*, FERMILAB-PROPOSAL-0989.
- [3] M. Benayoun, *et al.*, [arXiv:1407.4021].
- [4] T. Aoyama, M. Hayakawa, T. Kinoshita and M. Nio, *Phys. Rev. Lett.* **109** (2012) 111808 [arXiv:1205.5370].
- [5] M. Davier *et al.*, *Eur. Phys. J. C* **71** (2011) 1515 [Erratum-ibid. *C* **72** (2012) 1874] [arXiv:1010.4180].
- [6] K. Hagiwara *et al.* *J. Phys. G* **38** (2011) 085003 [arXiv:1105.3149].
- [7] M. Benayoun, P. David, L. DelBuono and F. Jegerlehner, *Eur. Phys. J. C* **73** (2013) 2453 [arXiv:1210.7184].
- [8] F. Jegerlehner and R. Szafron, *Eur. Phys. J. C* **71** (2011) 1632 [arXiv:1101.2872].
- [9] T. Blum, *Phys. Rev. Lett.* **91** (2003) 052001 [arXiv:hep-lat/0212018].
- [10] M. Göckeler *et al.*, *Nucl. Phys. B* **688** (2004) 135 [arXiv:hep-lat/0312032].
- [11] C. Aubin and T. Blum, *Phys. Rev. D* **75** (2007) 114502 [arXiv:hep-lat/0608011].
- [12] X. Feng, K. Jansen, M. Petschlies and D. B. Renner, *Phys. Rev. Lett.* **107** (2011) 081802 [arXiv:1103.4818].
- [13] P. Boyle, L. Del Debbio, E. Kerrane and J. Zanotti, *Phys. Rev. D* **85** (2012) 074504 [arXiv:1107.1497].
- [14] M. Della Morte, B. Jäger, A. Jüttner and H. Wittig, *JHEP* **1203** (2012) 055 [arXiv:1112.2894].
- [15] F. Burger *et al.* [ETM Collaboration], *JHEP* **1402** (2014) 099 [arXiv:1308.4327].
- [16] E. de Rafael, *Phys. Lett. B* **322** (1994) 239 [arXiv:hep-ph/9311316].
- [17] B. Chakraborty *et al.*, [arXiv:1403.1778].
- [18] P. F. Bedaque, *Phys. Lett. B* **593** (2004) 82 [arXiv:nucl-th/0402051].
- [19] G. M. de Divitiis, R. Petronzio and N. Tantalo, *Phys. Lett. B* **595** (2004) 408 [arXiv:hep-lat/0405002].
- [20] C. T. Sachrajda and G. Villadoro, *Phys. Lett. B* **609** (2005) 73 [arXiv:hep-lat/0411033].
- [21] H. Horch, G. Herdoíza, B. Jäger, H. Wittig, M. Della Morte and A. Jüttner, *PoS LATTICE* **2013** (2013) 304 [arXiv:1311.6975].
- [22] E. B. Gregory *et al.*, [arXiv:1311.4446].
- [23] C. Aubin, T. Blum, M. Golterman and S. Peris, *Phys. Rev. D* **88**, no. 7, 074505 (2013) [arXiv:1307.4701].
- [24] C. Aubin, T. Blum, M. Golterman and S. Peris, *Phys. Rev. D* **86** (2012) 054509 [arXiv:1205.3695].
- [25] M. Golterman, K. Maltman and S. Peris, *Phys. Rev. D* **88** (2013) 114508 [arXiv:1309.2153].
- [26] M. Golterman, K. Maltman and S. Peris, [arXiv:1405.2389].
- [27] M. Golterman, K. Maltman and S. Peris, [arXiv:1410.8405].
- [28] G. M. de Divitiis, R. Petronzio and N. Tantalo, *Phys. Lett. B* **718** (2012) 589 [arXiv:1208.5914].
- [29] S. L. Adler, *Phys. Rev. D* **10** (1974) 3714.
- [30] A. De Rújula and H. Georgi, *Phys. Rev. D* **13** (1976) 1296.
- [31] F. Jegerlehner, *Springer Tracts Mod. Phys.* **226** (2008) 1.
- [32] B. E. Lautrup, A. Peterman and E. de Rafael, *Phys. Rept.* **3** (1972) 193.
- [33] D. B. Renner, X. Feng, K. Jansen and M. Petschlies, *PoS LATTICE* **2011** (2012) 022 [arXiv:1206.3113].
- [34] A. Francis, B. Jäger, H. B. Meyer and H. Wittig, *Phys. Rev. D* **88** (2013) 054502 [arXiv:1306.2532].
- [35] M. Della Morte *et al.*, *PoS LATTICE* **2014** (2014) 162 [arXiv:1411.1206].
- [36] E. de Rafael, *Phys. Lett. B* **736** (2014) 522 [arXiv:1406.4671].
- [37] D. Bernecker and H. B. Meyer, *Eur. Phys. J. A* **47** (2011) 148 [arXiv:1107.4388].
- [38] X. Feng *et al.*, *Phys. Rev. D* **88** (2013) 034505 [arXiv:1305.5878].
- [39] A. Francis *et al.*, [arXiv:1410.7491].
- [40] A. Francis, V. Gülpers, B. Jäger, H. Meyer, G. von Hippel and H. Wittig, *PoS LATTICE* **2014** (2014) 128 [arXiv:1411.7592].
- [41] T. Blum, T. Izubuchi and E. Shintani, *Phys. Rev. D* **88** (2013) 9, 094503 [arXiv:1208.4349].
- [42] E. Shintani, *PoS LATTICE* **2014** (2014) 124.
- [43] B. Colquhoun *et al.*, [arXiv:1408.5768].
- [44] F. Burger *et al.*, *PoS LATTICE* **2013** (2013) 301 [arXiv:1311.3885].
- [45] M. Della Morte, B. Jäger, A. Jüttner and H. Wittig, *PoS LATTICE* **2012** (2012) 175 [arXiv:1211.1159].
- [46] <http://www-com.physik.hu-berlin.de/~fjeger/software.html>
- [47] G. Herdoíza, H. Horch, B. Jäger and H. Wittig, *PoS LATTICE* **2013** (2014) 444.
- [48] A. Francis, G. Herdoíza, H. Horch, B. Jäger, H. B. Meyer and H. Wittig, *PoS LATTICE* **2014** (2014) 163 [arXiv:1412.6934].
- [49] M. Della Morte and A. Jüttner, *JHEP* **1011** (2010) 154 [arXiv:1009.3783].
- [50] E. Shintani, talk at this conference (2014).